Performance Improvement in Semi-dry Ozone Injection NO_x and SO_x Removal Process for a Glass Furnace Flue Gas

Yuta Fukuda[1], Tomoyuki Kuroki[1], Ryosuke Nishioka[1], Hidekatsu Fujishima[1],

Haruhiko Yamasaki[1], Hashira Yamamoto[2], and Masaaki Okubo[1]

[1]Department of Mechanical Engineering, Osaka Prefecture University, 1-1 Gakuen-cho,

Naka-ku, Sakai 599-8531, Japan

[2]Environmental Affairs Office, Nihon Yamamura Glass Co., Ltd., Amagasaki, Hyogo 660-8580,

Japan

Address correspondence to Tomoyuki Kuroki, Department of Mechanical Engineering, Osaka Prefecture University, 1-1 Gakuen-cho, Naka-ku, Sakai 599-8531, Japan.

Email: kuroki@me.osakafu-u.ac.jp

Abstract

A combined ozone injection and semi-dry chemical NO_x and SO_x removal process using nonthermal plasma for the treatment of flue gases emitted from glass melting furnaces has been proposed. To further improve the NO_x removal, O_3 was injected in directions opposite to the direction of gas flow at the center of the semi-dry reactor. Moreover, the effect of the increase in initial concentrations of NO and SO_2 was investigated. In addition, the effect of the gas flow rate on NO oxidation, denitration, and desulfurization efficiencies, and the effect of NaOH and SO_3^{2-} concentrations on denitration and desulfurization efficiencies were investigated.

Keywords Ozone, Glass melting furnace, Nonthermal plasma, NO_x, SO_x, Semi-dry process

INTRODUCTION

In glass bottle manufacturing plants, a large amount of fossil fuel, such as heavy oil and city gas is combusted to melt the raw material of glass. Thus, nitrogen oxides (NO_x = nitric oxide (NO) and nitrogen dioxide (NO_2)) that are mainly derived from high-temperature combustion, and sulfur oxide (SO_x, mainly sulfur dioxide (SO_2)) derived from fuel and raw material of glass are emitted from glass melting furnaces. SO_2 is generally treated by wet or semi-dry desulfurization reactors with sodium hydroxide (NaOH) aqueous solution because it is easily absorbed by NaOH aqueous solution (Zhou et al. 2017), and the sodium sulfate (Na_2SO_4) generated by SO_2 absorption is available as a raw glass material (Min'ko and Binaliev 2013). Sodium sulfite (Na_2SO_3) and Na_2SO_4 from the desulfurization equipment were collected by electrostatic precipitators and bag filters placed downstream of the desulfurization reactor. However, there is no method for effective NO_x removal for glass melting furnaces. Selective catalytic reduction (SCR) (Li et al. 2011), a conventional NO_x removal method, is widely used for thermal power stations, factories, automobiles, and ships, but it is difficult to use SCR in glass melting furnaces. This is because the sodium compound in the exhaust gas (formed by the reaction of sulfur oxide and alkali) causes catalyst poisoning (Yang et al. 2013). In addition to SCR, although there is a wet process involving NO oxidation and NO_2 absorption by water or an alkali aqueous solution, the wet process is significantly more complex than a dry process such as SCR, and it is difficult to achieve both higher efficiency and lower cost using the wet process (Yamamoto et al. 2000). For the reasons stated previously, NO_x emissions from glass melting furnaces are controlled by either using a low NO_x burner (Noda et al. 2007) or reducing

combustion air to less than the theoretical air. However, it is difficult to significantly reduce NO_x emissions using this method (Uejima et al. 2005), as it results in fuel loss and a high concentration of carbon monoxide (CO). Therefore, a novel NO_x aftertreatment method applicable to glass melting furnaces is required.

A novel method using atmospheric pressure nonthermal plasma (NTP) for NO_x removal for boilers, diesel engines, and garbage incinerators has been investigated and proposed (Cha et al. 2007; Chang et al. 1998; Chang et al. 2004; Dinelli et al. 1990; Hayakawa et al. 2016; Meng et al. 2019; Mok and Lee 2006; Nishanth and Rajanikanth 2021; Oda et al. 1998; Sano and Yoshioka 2003; Si et al. 2019; Zhou et al. 1992; Zhou et al. 2016). We previously reported (Fujishima et al. 2013) that NO_x from a boiler could be effectively removed using the wet plasma-chemical hybrid method that combines NO oxidation with NTP induced ozone (O_3) and NO_2 reduction using Na_2SO_3 aqueous solution. As this method does not require a catalyst, there is no risk of catalyst poisoning. In addition, this method is easily adapted to existing desulfurization reactors. We have previously demonstrated that this method can be used successfully for wet desulfurization reactors (Yamamoto et al. 2016a).

When a semi-dry desulfurization reactor is used, the gas temperature at the outlet of the reactor must be maintained above 200°C, because the droplets of NaOH aqueous solution sprayed in the reactor must be completely dry for electrostatic precipitator and bag filters placed downstream of the reactor to operate properly. Semi-dry desulfurization reactors are more widely used than wet desulfurization reactors because they require a lower flow rate of NaOH aqueous solution and do not require complex control of aqueous solution and wastewater treatment. However, the oxidation efficiency of NO is significantly reduced at temperatures greater

than 150°C (Fujishima et al. 2013). To successfully apply the plasma-chemical hybrid method to a semi-dry desulfurization reactor, O_3 must be efficiently injected and spread throughout the localized cooling area created by cooling water or solution spray. Using a laboratory-scale model that is 1/50000 the size of the actual semi-dry desulfurization reactor, we demonstrated that NO can be effectively oxidized by injecting O_3 into the localized cooling area (Kuroki et al. 2014; Yamamoto et al. 2016b; Yamamoto et al. 2016c; Yamamoto et al. 2019; Yamasaki et al. 2021). A liquid-to-gas ratio (L/G) greater than 20 times that of the actual reactor was used to achieve NO removal efficiency of 89% and NO_x removal efficiency of 61% (Kuroki et al. 2014). Furthermore, when the NO_x and SO_x were removed simultaneously, the NO removal efficiency of 90%, NO_x removal efficiency of 50%, and SO_2 removal efficiency of 84% were obtained (Yamamoto et al. 2016b). However, when the L/G was reduced to 0.7 that is seven times of that of the actual reactor, NO, NO_x, and SO_2 removal efficiencies were 62%, 45%, and 80%, respectively, and the NO removal efficiency was significantly reduced despite the localized cooling area (Yamamoto et al. 2016c). This is because O_3 was injected vertically into the gas flow at the center of the semi-dry reactor, and some of the O_3 escaped from the localized cooling area, i.e., was decomposed. Hence, in a previous study (Yamasaki et al. 2021), the O_3 injection position was shifted from the reactor's center to the inner wall of the reactor. The results indicate that the efficiencies of NO, NO_x, and SO_2 removal were increased and were 98%, 68%, and 100%, respectively. In this study, to further improve the NO_x removal efficiency by increasing the contact time between NO_2 generated by NO oxidation and Na_2SO_3 generated by SO_2 absorption of NaOH, O_3 was injected in opposite directions to the gas flow at the center of

the semi-dry reactor and NO oxidation was caused upstream of O_3 injection point. Moreover, the initial concentrations of NO and SO_2 were increased from 100 ppm to 300 ppm because the actual concentrations of NO and SO_2 were close to 300 ppm, and the effect of the increase in initial concentrations of NO and SO_2 was investigated. In addition, the effect of gas flow rate on NO oxidation, denitration, and desulfurization efficiency was investigated, as well as the effect of NaOH and SO_3^{2-} concentrations on denitration and desulfurization efficiency. Furthermore, the N_2O concentration in the treated gas was measured because N_2O could be generated as a byproduct of NO_2 reduction process. Consequently, the optimal conditions for the simultaneous removal of NO_x and SO_2 were determined.

PRINCIPLE OF NO_x AND SO_2 REMOVAL IN SEMI-DRY EQUIPMENT

The plasma-chemical hybrid process for NO_x and SO_2 removal combines plasma and chemical processes. In the plasma process, NO is oxidized to NO_2 by O_3 induced by the NTP, as shown in Reaction (1).

$$NO + O_3 \rightarrow NO_2 + O_2 \quad (1)$$

This oxidation reaction occurs rapidly (Atkinson et al. 2004), whereas the oxidation efficiency of NO decreases when the gas temperature exceeds 150°C. For effective NO oxidation, O_3 should be injected into a localized cooling area of less than 150°C induced by the solution spray. In contrast, because the reaction between O_3 and SO_2 is extremely slow (DeMore et al. 1997) when NO coexists with SO_2, O_3 reacts selectively with NO (Nelo et al. 1997).

In the chemical process, SO_2 is absorbed by NaOH solution spray droplets to yield Na_2SO_3 as a byproduct, as shown in Reaction (2). Na_2SO_3 is a strong reducing agent that can reduce NO_2 to N_2, as shown in Reaction (3).

$$SO_2 + 2NaOH \rightarrow Na_2SO_3 + H_2O \quad (2)$$

$$2NO_2 + 4Na_2SO_3 \rightarrow N_2 + 4Na_2SO_4 \quad (3)$$

Both reactions (2) and (3) are gas–liquid reactions, and thus must be carried out before the spray droplets are completely dry.

EXPERIMENTAL SETUP AND METHODS

In this study, a laboratory-scale model that is 1/50000 the size of an actual semi-dry desulfurization reactor was used. **Figure 1** shows a schematic of the experimental setup. The simulated flue gas was generated using cylinders of N_2-based NO and SO_2 mixed gas (NO = 1000 ppm, SO_2 = 1000 ppm), N_2 and O_2 mixed gas (N_2 =79%, O_2 =21%), and N_2 gas. The flow rate and the concentrations of NO, SO_2, and O_2 were regulated by mass flow controllers (SFC280E, Hitachi Metals, Ltd., Japan). The flue gas flow rate was set to between 5 to 15 L/min, and the NO, SO_2, and O_2 concentrations were set at 300 ppm, 300 ppm, and 10%, respectively. After the gas was heated in a tube furnace (EKK-122K, Isuzu Seisakusho Co., Ltd., Japan), it was introduced into the reactor. O_3 was generated by a surface-discharge-type ozone generator (Ozonizer, OZS-EPIII-05, Masuda Research Inc., Japan) equipped with a 99.5% O_2 cylinder. The O_3 concentration was measured using an

ultraviolet absorbance ozone monitor (EG-550, Ebara Jitsugyo Co., Ltd., Japan). The generated O_3 was injected into the reactor, and the injected O_3 oxidized NO to NO_2. The concentration of O_3 gas was 33 g/m^3, and the flow rate of O_3 gas was varied between 0.1–0.3 L/min depending on the flue gas flow rate. A mixed NaOH and Na_2SO_3 aqueous solution was prepared by dissolving Na_2SO_3 powder (Special grade, Kishida Chemical Co., Ltd., Japan) and NaOH solution (0.5 mol/L, Kishida Chemical Co., Ltd., Japan) in pure water. The concentrations of NaOH and SO_3^{2-} were set in the ranges of 0.15%–0.30% and 0%–1.2%, respectively. Next, SO_2 and NO_2 were treated by spraying NaOH and Na_2SO_3 aqueous solution from an 18-L stainless steel pressure tank (TM18SRV, Unicontrols Co., Ltd., Japan) at a gauge pressure of 0.45 MPa using a N_2 cylinder. The spray flow rate was set to 7 mL/min. NaOH absorbs SO_2 generating Na_2SO_3. NO_2 was then reduced to N_2 by Na_2SO_3. Subsequently, the treated gas was discharged from the outlet at the upper part of the reactor. Most of the sprayed aqueous solution was dried in the semi-dry equipment, while the residue was drained from an overflow tube attached to the lower part of the reactor, and the flue gas was analyzed downstream of the reactor. The NO_x, NO, O_2, SO_2, and N_2O concentrations were measured using a portable gas analyzer (PG-350, Horiba, Ltd., Japan) and a N_2O analyzer (VIA-510, Horiba, Ltd., Japan). The experiments were conducted more than once for each experimental condition to confirm their reproducibility.

Figure 2 shows the details of the laboratory-scale semi-dry desulfurization reactor combined with O_3 injection. It is cylindrical in shape, with an inner diameter of 56 mm, and a height of 1000 mm, and is made of

SUS304. After aligning the z-axis with the reactor's vertical axis (upward: +), the simulated flue gas inlet was placed at z = 0 mm. The spray position was varied between z = 150–500 mm, and a gas outlet was provided at z = 600 mm. The spray position adjustments were made by changing the position of the spray nozzle. A 435 mm long jacket heater (Eikou Electric Co., Ltd.: voltage of 100 V, power of 500 W) was attached to the reactor outer surface's upper row, and a 400 mm long jacket heater (Eikou Electric Co., Ltd.: voltage of 100 V, power of 450 W) was attached to the reactor outer surface's bottom row in order to maintain the temperature of the reactor wall surface constant by PID control. These two rows of heaters were also used to heat the gas inside the reactor and simulate the high-temperature exhaust gas conditions (greater than 200°C) found inside the actual semi-dry desulfurization reactor. Furthermore, an O_3 injection tube with a closed tip and a hole in the side wall, as shown in Fig. 2, is placed at z = 100 mm, allowing O_3 to be injected in the opposite direction of the simulated flue gas flow at the center of the reactor. The gas temperature was measured at z = 0, 100, 200, 250, 300, 350, 400, 450, 500, 550, and 600 mm. For the measurement points of z = 0 (inlet), 200, and 600 mm (outlet), the gas temperature was measured using thermocouples fixed to the reactor throughout all experiments. The gas temperature at the measurement point, except for the specific points mentioned previously, was measured using a movable thermocouple in the vertical direction; a thermocouple temporarily replaced by the O_3 injection tube, was employed only when the gas temperature distribution in the reactor was investigated.

RESULTS AND DISCUSSION

Measurement of Gas Temperature Distribution in the Semi-dry Reactor

To keep NO oxidation by O_3 from deteriorating, it is critical to create a localized cooling area of less than 150°C in the reactor by spraying solution and injecting O_3. In addition, because NO_2 reduction by Na_2SO_3 is a gas–liquid reaction, it is desirable to spread in as widely as possible, a localized cooling area with gas temperature less than 100°C and a high concentration of solution droplets, while maintaining a gas temperature greater than 200°C at the reactor outlet. To gain a better understanding of the temperature distribution of gas in the reactor, we first measured the gas temperature at each measurement point as the spray position was changed. **Figure 3** shows the vertical distribution of gas temperature for each spray position at a spray flow rate of 7 mL/min and a gas flow rate of 10 L/min. When the spray position is in the range of 150–400 mm, the gas inlet (z = 0 mm) and the O_3 injection position (z =100 mm) temperatures are cooled to less than 150°C. However, they are over 150°C and are not sufficiently cooled when the spray positions are 450 and 500 mm. In the gas–liquid reaction, the distance between the gas inlet and the spray position should be as large as possible because the residence time of the flue gas in an area with a large number of droplets should be longer. Therefore, the spray position was set to z = 400 mm.

Effects of the Concentrations of NaOH and SO_3^{2-} on NO_x and SO_x removal

The removal efficiencies of NO (η_{NO}), NO_x (η_{NOx}), and SO_2 (η_{SO2}) were determined when the concentrations of NaOH and SO_3^{2-} were varied. Gas concentrations were measured every 5 min for a total of 20 min for each condition during the experiment. **Figure 4** shows the removal efficiencies of NO, NO_x, and SO_2 as a function of the NaOH concentration. The flow rates of flue gas and O_2 supplied to the ozonizer were set to

10 and 0.2 L/min, respectively. The SO_3^{2-} concentration was 0%. Each point and error bar in the figure denotes the mean value of four measurements and their standard deviations. According to Reaction (2), a 0.15% NaOH concentration is required to completely absorb SO_2. In addition, SO_3^{2-} generated by this reaction reduces NO_2 by 150 ppm. From the figure, regardless of the NaOH concentration, the NO removal efficiency of 92–95% is obtained. Although O_3 is decomposed by NaOH (von Gunten 2003), the NaOH concentration of 0.15% to 0.30% had no effect on NO removal efficiency. The SO_2 removal efficiency of 88% is attained when the NaOH concentration is 0.15%, and the SO_2 removal efficiency increases with increasing NaOH concentration, resulting in the SO_2 removal efficiency of 98% when the NaOH concentration is 0.30%. The NO_x removal efficiency is 58% when the NaOH concentration is 0.15%; however, the NO_x removal efficiency decreases slightly with increasing NaOH concentration, and the NO_x removal efficiency decreases to 50% when the NaOH concentration is 0.30%. The HSO_3^-, generated when NaOH is insufficient to absorb SO_2, reacts with NO_2 of 2 mol per 1 mol of HSO_3^- (Cai et al. 2020). The amount of removed NO_2 decreases because the HSO_3^- concentration decreases with increasing NaOH concentration. Thus, it is assumed that the NO_x removal efficiency decreases. The optimal concentration of NaOH is 0.20% upon considering the removal efficiencies of SO_2 and NO_x, and operating costs.

Figure 5 shows the removal efficiencies of NO, NO_x, and SO_2 plotted as functions of SO_3^{2-} concentration. The flow rates of flue gas and O_2 supplied to the ozonizer were set to 10 and 0.2 L/min, respectively. The NaOH concentration was 0.20%. The NO removal efficiency of 93–97% is obtained regardless of SO_3^{2-} concentration,

which is varied between 0–1.2%. The SO_2 removal efficiency of more than 95% was achieved when the SO_3^{2-} concentration was in the range of 0–1.0%; however, the SO_2 removal efficiency slightly decreases when the SO_3^{2-} concentration is 1.2%. The NO_x removal efficiency with an SO_3^{2-} concentration of 0.15% is greater than the concentration with SO_3^{2-} of 0%, and it is almost stable when the SO_3^{2-} concentration is in the range of 0.15–0.8%. When SO_3^{2-} concentration is 0%, HNO_2 and HNO_3 can be generated because of lack of SO_3^{2-}. In addition, some SO_3^{2-} can react with O_2 ; therefore, the NO_x removal efficiency may be stable. The NO_x removal efficiency increases to 70% when the SO_3^{2-} concentration is 1.0%; however, it decreases when the SO_3^{2-} concentration is 1.2%. It is believed that the decrease in the removal efficiencies of NO, SO_2, and NO_x with the SO_3^{2-} concentration of 1.2% was caused by the clogging of holes in the spray nozzle with increase in solution viscosity. The results show that the optimum SO_3^{2-} concentration is 1.0% for obtaining maximum NO_x removal efficiency.

Effect of the Flue Gas Flow Rate on Denitration and Desulfurization

To evaluate the effect of flue gas flow rate on denitration and desulfurization, NO, NO_x, SO_2, and N_2O concentrations were measured when the gas flow rate was set at 5, 6, 10, and 15 L/min. The flow rate of the spray solution was 7 mL/min. The gas flow rates of 5, 6, 10, and 15 L/min had L/G values of 1.40, 1.17, 0.70, 0.47 L/m^3, respectively. The NaOH and SO_3^{2-} concentrations of the spray solution were set to 0.20 and 1.0%, respectively. The O_2 flow rates supplied into ozonizer were set to 0.10, 0.12, 0.20, and 0.30 L/min, respectively depending on the flue gas flow rate, in order to maintain a molar ratio of O_3 to NO of 1.0. Fig. 6 shows the

concentrations of NO, NO_x, SO_2, O_2, and N_2O as a function of the elapsed time when the flue gas flow rates were 5, 6, 10, and 15 L/min. The O_3 injection was initiated at 5 min. Fig. 7 shows the gas temperature at z = 0 mm (the gas inlet), 200 mm, and 600 mm (the gas outlet) as a function of the elapsed time when the experiment shown in Fig. 6 was conducted. Figs. 6(a) and 7(a) show the results obtained when the flue gas flow rate was 5 L/min. As shown in Fig. 6(a), the NO concentration decreases from 306 ppm to 2 ppm, and NO removal efficiency of 99% is achieved. The NO_x concentration also decreases from 331 ppm to 46 ppm with the decrease in NO, resulting in NO_x removal efficiency of 86%. In contrast, owing to the SO_2 absorption by NaOH, the SO_2 concentration is maintained at 0 ppm regardless of the O_3 injection. Because N_2O generation is less than 1 ppm, it can be considered negligible. As shown in Fig. 7(a), the gas temperature at the gas inlet (z = 0 mm), z = 200 mm, and gas outlet (z = 600 mm) is 71, 76, and 245°C, respectively, and the solution spray forms a localized cooling area around the O_3 injection point. When the flue gas flow rate is increased to 6 L/min, nearly identical results to those at 5 L/min are obtained, as shown in Figs. 6(b) and 7(b). When the flue gas flow rate is increased to 10 L/min, as shown in Fig. 6(c), the NO concentration decreases from 297 ppm to 23 ppm, and NO removal efficiency of 92% is attained. The NO_x concentration also decreases from 318 ppm to 99 ppm, NO_x removal efficiency of 69% is obtained. As shown in Fig. 7(c), the gas temperature at the gas inlet (z = 0 mm), z = 200 mm, and the gas outlet (z = 600 mm) are 120, 96, and 224°C, respectively, and the gas temperature of the localized cooling area is greater than that at 5 and 6 L/min. Therefore, the NO removal efficiency decreases. In addition, the NO_x removal efficiency decreases further as the L/G ratio decreases. Furthermore, the SO_2

concentration decreases to only 7 ppm. The amount of N_2O generated is approximately 2 ppm. Figs. 6(d) and 7(d) show the results obtained with a flue gas flow rate of 15 L/min. As shown in Fig. 6(d), the NO concentration decreases from 306 ppm to 26 ppm, achieving NO removal efficiency of 92%. The NO_x concentration also decreases from 326 ppm to 149 ppm, resulting in NO_x removal efficiency of 54%. As shown in Fig. 7(d), the gas temperature at the gas inlet (z = 0 mm), z = 200 mm, and the gas outlet (z = 600 mm) are 163, 90, and 221°C, respectively. Although the temperature at the gas inlet (z = 0 mm) is higher than the temperature at 10 L/min, the NO removal efficiency is comparable. It is assumed that the gas temperature at the O_3 injection point is cooled to the same level as at 10 L/min, and the injected O_3 reacts rapidly with NO. However, the NO_x removal efficiency is significantly affected by the decrease in L/G ratio. The SO_2 concentration decreases to 28 ppm. The N_2O generation is 6 ppm, which increases with the flue gas flow rate when 5, 6, and 10 L/min are used. This is probably because decreasing the L/G ratio decreases SO_2 removal efficiency, and some of the SO_2 is oxidized to SO_3 by O_3, which then SO_3 reacts with NO (Nishida et al. 2005).

To evaluate the effect of O_3 injection on NO oxidation, the NO oxidation efficiency defined as the molar ratio of the decreased NO to the injected O_3 ($\Delta NO/O_3$) was obtained. Fig. 8 shows $\Delta NO/O_3$ plotted as a function of the flue gas flow rate. The results of a previous study (Yamasaki et al. 2021) are also included for comparison. They were obtained using O_3 injection from the inner wall of the reactor and the initial NO and SO_2 concentrations of 100 ppm. Each point and error bar in the figure represent the mean value of four measurements that were taken every 5 min over the course of the 20-min experiment, as well as their standard deviations.

When the flue gas flow rate is between 5 and 6 L/min, $\Delta NO/O_3$ ratio reaches approximately 100%, which means that almost all of the injected O_3 reacted with NO. However, when the flue gas flow rates are 10 and 15 L/min, the $\Delta NO/O_3$ is 91 and 93%, respectively. It is assumed that as L/G ratio decreases, the area of sufficiently cooled decreases, as the temperature differential between the gas inlet and z = 200 mm becomes large, as shown in Fig. 7(c) and 7(d). The previous findings show that when the flue gas flowrate is 5 L/min and 15 L/min, $\Delta NO/O_3$ ratio decreases owing to insufficient dispersion of O_3 in localized cooling. By contrast, mixing of NO and O_3 is facilitated, and the $\Delta NO/O_3$ ratio is increased by injecting O_3 in the opposite direction of gas flow in the center of the reactor.

To evaluate the NO_2 removal by solution spray, the decreasing ratio of NO_2 was defined as the molar ratio of the decreased NO_x to the decreased NO ($\Delta NO_x/\Delta NO$). Δ NO is equivalent to NO_2 produced by the reaction of NO with O_3. Figure 9 shows the $\Delta NO_x/\Delta NO$ ratio and NO_x removal efficiency plotted as functions of the flue gas flow rate. The results of the previous study (Yamasaki et al. 2021) are also shown in Fig. 9 for comparison. Each point and error bar in the figure represents the mean value of four measurements taken every 5 min during the 20 min experimental period, as well as their standard deviations. The $\Delta NO_x/\Delta NO$ ratio increases as the flue gas flow rate decreases, reaching 94% at a flue gas flow rate of 5 L/min. This is because L/G ratio and contact time between NO_2 and Na_2SO_3 increases as the flue gas flow rate decreases. The NO_x removal efficiency at 5 L/min is slightly lower than at 6 L/min owing to the slightly higher initial NO_x concentration at 5 L/min; however, the removed NO_x is nearly identical at both flow rates. The NO_x removal

efficiency also increases as the flue gas flow rate decreases, reaching 88% at a flue gas flow rate of 6 L/min. Based on the above results, the optimal flue gas flow rate within the range of the flue gas flow rate in this study was 6 L/min.

Furthermore, while the $\Delta NO_x/\Delta NO$ ratio and NO_x removal efficiency are similar to those found in the previous study at a flue gas flow rate of 15 L/min, they are significantly improved over those found in the previous study at a flue gas flow rate of 6 L/min. The results show that when L/G ratio is high, the improvement of the O_3 injection method is effective for $\Delta NO_x/\Delta NO$ and NO_x removal efficiency because sufficient contact time between NO_2 and Na_2SO_3 is obtained.

CONCLUSIONS

To improve the performance of NO_x and SO_x removal, an improved O_3 injection method using a combination of plasma and semi-dry chemical processes for flue gas treatment from a glass melting furnace was investigated. In addition, the effect of the gas flow rate on NO oxidation, denitration, and desulfurization efficiencies, and the effect of NaOH and SO_3^{2-} concentrations on denitration and desulfurization efficiencies were investigated. The results are summarized as follows:

(1) The vertical temperature distribution of the gas was measured as the spray position was changed, and it was determined that when the spray position was 400 mm, distance between the gas inlet and spray position was enlarged the most, while forming a localized cooling area of less than 150°C around the O_3 injection point.

(2) When the NaOH concentration was varied between 0.15 to 0.30%, the NO removal efficiency was

almost stable regardless of the NaOH concentration and the SO_2 removal efficiency increased as NaOH concentration increased. However, the NO_x removal efficiency decreased slightly as NaOH concentration increased. Taking into account the removal efficiencies of SO_2 and NO_x, and operating costs, the optimal concentration of NaOH is 0.20%.

(3) When the SO_3^{2-} concentration was varied in the range of 0–1.2%, the NO removal efficiency remained almost constant regardless of the SO_3^{2-} concentration. The SO_2 removal efficiency was also nearly stable. The NO_x removal efficiency increased and reached 70% when the SO_3^{2-} concentration was 1.0%. However, when the SO_3^{2-} concentration was 1.2%, the removal efficiencies of NO, SO_2, and NO_x decreased. The results showed that the optimal concentration of SO_3^{2-} was 1.0%.

(4) $\Delta NO/O_3$ ratio was significantly improved in this study by injecting O_3 in the opposite direction of the flue gas flow at the center of the reactor. When the flue gas flow rate was 5 L/min and 6 L/min, $\Delta NO/O_3$ ratio reached nearly 100%.

(5) Although the $\Delta NO_x/\Delta NO$ ratio and NO_x removal efficiency were both improved by the improvement of the O_3 injection method when the flue gas flow rate was between 5 and 6 L/min, the effect of the improvement of the O_3 injection method was hardly confirmed because of the decreasing residence time in the reactor when the flue gas flow rate was greater than 10 L/min.

ACKNOWLEDGMENTS

We would like to thank Mr. Y. Mizuguchi and Mr. R. Kinoshita, who were students at Osaka Prefecture University at the time this study was conducted. This study was subsidized by a project fund (Strategic Innovation Program for Energy Conservation Technologies: JPNP12004) of the New Energy and Industrial Technology Development Organization (NEDO).

REFERENCES

Atkinson, R., D. L. Baulch, R. A. Cox, J. N. Crowley, R. F. Hampson, R. G. Hynes, M. E. Jenkin, M. J. Rossi, and J. Troe. 2004. "Evaluated Kinetic and Photochemical Data for Atmospheric Chemistry: Volume I – Gas Phase Reactions of O_x, HO_x, NO_x and SO_x Species." Atmospheric Chemistry and Physics 4: 1461–738.

Cai, M., X. Liu, T. Zhu, Y. Zou, W. Tao, and M. Tian. 2020. "Simultaneous Removal of SO_2 and NO Using a Spray Dryer Absorption (SDA) Method Combined with O_3 Oxidation for Sintering/Pelleting Flue Gas." Journal of Environmental Science 96: 62-71.

Cha, M. S., Y. H. Song, J. O. Lee, and S. J. Kim. 2007. "NO_x and Soot Reduction Using Dielectric Barrier Discharge and NH_3 Selective Catalytic Reduction in Diesel Exhaust." International Journal of Plasma Environmental Science and Technology 1(1): 28–33.

Chang, J. S., K. Urashima, M. Arquillq, and T. Ito. 1998. "Reduction of NO_x from Combustion Flue Gases by Corona Discharge Activated Methane Radical Injections." Combustion Science and Technology 133(1–3):

31–47.

Chang, M. B., H. M. Lee, F. Wu, and C. Lai. 2004. “Simultaneous Removal of Nitrogen Oxide/Nitrogen Dioxide/Sulfur Dioxide from Gas Streams by Combined Plasma Scrubbing Technology.” Journal of the Air & Waste Management Association 54(8): 941–9.

DeMore, W. B., D. M. Golden, R. F. Hampson, C. J. Howard, C. E. Kolb, and M. J. Molina. 1997. “Chemical Kinetics and Photochemical Data for Use in Stratospheric Modeling”, JPL Publication, Evaluation number 12, Vol. 97–4.

Dinelli, G., L. Civitano, and M. Rea. 1990. “Industrial Experiments on Pulsed Corona Simultaneous Removal of NO_x and SO_2 from Flue Gas.” IEEE Transactions on Industry Applications 26(3): 535–41.

Fujishima, H., K. Takekoshi, T. Kuroki, A. Tanaka, K. Otsuka, and M. Okubo. 2013. “Towards Ideal NO_x Control Technology for Bio-oils and a Gas Multi-fuel Boiler System Using a Plasma-chemical Hybrid Process.” Applied Energy 111: 394–400.

Hayakawa, Y., Y. Inoue, A. Takeyama, and S. Kambara. 2016. “Reaction Mechanism of De-NO_x by Activated Ammonia Generated by Dielectric Barrier Discharge.”, International Journal of Plasma Environmental Science & Technology 10(1): 20–3.

Kuroki, T., H. Yamamoto, H. Fujishima, D. Takada, Y. Yamato, and M. Okubo. 2014. “NO_x Removal for Flue Gas in Glass Furnace Using an Ozone Injection Chemical Hybrid Process–Laboratory Experiments with Semi-Dry Model System–.” Journal of the Institute of Electrostatics Japan 38: 52–8 (In Japanese).

Li, J., H. Chang, L. Ma, L. Hao, and R. T. Yang. 2011. “Low-temperature Selective Catalytic Reduction of NO_x with NH_3 over Metal Oxide and Zeolite Catalysts—A review.” Catalysis Today 175(1): 147–56.

Meng, Z., C. Wang, X. Wang, Y. Chen, W. Wu, and H. Lia. 2019. “Simultaneous Removal of SO_2 and NO_x from Flue Gas Using $(NH_4)_2S_2O_3$/Steel Slag Slurry Combined with Ozone Oxidation.” Fuel 255: 115760.

Min’ko, N. I. and I. M. Binaliev. 2013. “Role of Sodium Sulfate in Glass Technology.” Glass and Ceramics 69(11–12): 361–5.

Mok, Y. S. and H. J. Lee. 2006. “Removal of Sulfur Dioxide and Nitrogen Oxides by Using Ozone Injection and Absorption–Reduction Technique.” Fuel Processing Technology 87(7): 591–7.

Nishanth, K. and B. S. Rajanikanth. 2021. “Red Mud Packed Surface Discharge Reactor for No_x/THC Removal: Exploring Plasma Catalysis of Diesel Exhaust.” Plasma Chemistry and Plasma Processing 41(5): 1293–311.

Nelo, S. K., K. M. Leskela, and J. J. K. Sohlo. 1997. “Simultaneous Oxidation of Nitrogen Oxides and Sulfur Dioxide with Ozone and Hydrogen Peroxide.” Chemical Engineering & Technology 20: 40–2.

Nishida, O., A. Sudrajad, H. Fujita, and W. Harano. 2005. “Study of Formation and Decomposition of Nitrous Oxide by Heating Reactor.” Journal of the Japan Institute of Marine Engineering 40(4): 103–6.

Noda, S., I. G. Parwatha, Y. Nada, S. Nishio, and S. Fukushige. 2007. “Effect of Flow Field on NO_x Emission Properties of Jet Nonpremixed Flames in Cylindrical Furnaces.” Journal of Environment and Engineering 2(4): 730–9.

Oda, T., T. Kato, T. Takahashi, and K. Shimizu. 1998. “Nitric Oxide Decomposition in Air by Using Non-thermal Plasma Processing-with Additives and Catalyst.” IEEE Transactions on Industry Applications 34(2): 268–72.

Sano, K. and Y. Yoshioka. 2013. “Effect of Oxygen Injection and HC Addition on NO Removability of Ozone Injection Method.” IEEJ Transaction on Fundamentals and Materials Society 123(10): 1030–6.

Si, T., C. Wang, X. Yan, Y. Zhang, Y. Ren, J. Hu, and E. J. Anthony. 2019. “Simultaneous Removal of SO_2 and NO_x by a New Combined Spray-and Scattered-bubble Technology Based on Preozonation: From Lab Scale to Pilot Scale.” Applied Energy 242: 1528–38.

Uejima, M., R. Iwaki, M. Wakimura, S. Noda, and Y. Onuma. 2005. “Premixing Combustion of a Lifted Non-Premixed Flame in Hot Airstreams and NO_x Reduction.” Transactions of the Japan Society of Mechanical Engineers B 71(701): 310–5 (In Japanese).

von Gunten, U. 2003. “Ozonation of Drinking Water: Part I. Oxidation Kinetics and Product Formation.” Water Research 37: 1443–67.

Yang, B., Y. Shen, S. Shen, and S. Zhu. 2013. “Regeneration of the Deactivated TiO_2-ZrO_2-CeO_2/ATS Catalyst for NH_3-SCR of NO_x in Glass Furnace.” Journal of Rare Earths 31(2): 130–6.

Yamamoto, T., C. L. Yang, Z. Kravets, and M. Beltran. 2000. “Plasma-assisted Chemical Process for NO_x Control.” IEEE Transactions on Industry Applications 36(3): 923–7.

Yamamoto, H., T. Kuroki, H. Fujishima, and M. Okubo. 2016a. “Pilot-scale Exhaust Gas Treatment for a Glass

Manufacturing System Using a Plasma Combined Wet Chemical Process." Mechanical Engineering Journal 3(1): Paper No.15-00549.

Yamamoto, Y., H. Yamamoto, D. Takada, T. Kuroki, H. Fujishima, and M. Okubo. 2016b. "Simultaneous Removal of NO_x and SO_x from Flue Gas of a Glass Melting Furnace Using a Combined Ozone Injection and Semi-dry Chemical Process." Ozone: Science & Engineering 38(3): 211–8.

Yamamoto, H., T. Kuroki, H. Fujishima, Y. Yamamoto, K. Yoshida, and M. Okubo. 2016c. "NO_x and SO_x Removals for Exhaust Gas in Glass Melting Furnace Using a Plasma and Dry Chemical Hybrid Process." Transactions of the Japan Society of Mechanical Engineers 82(843): 16–00255 (In Japanese).

Yamamoto, H., T. Kuroki, H. Fujishima, and M. Okubo. 2019. "Pilot-scale NO_x and SO_x Aftertreatment Using a Two-phase Ozone and Chemical Injection in Glass-melting-furnace Exhaust Gas." IEEE Transactions on Industry Applications 55(6): 6295–302.

Yamasaki, H., Y. Mizuguchi, K. Maeda, H. Fujishima, T. Kuroki, H. Yamamoto, and M. Okubo. 2021. "Performance Evaluation of Semi-dry Flue Gas Desulfurization and Denitration from Flue Gas of a Glass Melt Using Nonthermal Plasma Combined Process." Mechanical Engineering Journal 8(2): 20-00519.

Zhou, C., J. Zhou, Y. Feng, and Y. Zhu. 2016. "Marine Emission Pollution Abatement Using Ozone Oxidation by a Wet Scrubbing Method." Industrial & Engineering Chemistry Research 55(20): 5825−31.

Zhou, J., S. Zhou, and Y. Zhu. 2017. "Experiment and Prediction Studies of Marine Exhaust Gas SO_2 and Particle Removal Based on NaOH Solution with a U-type Scrubber." Industrial & Engineering Chemistry

Research 56(43):12376–84.

Zhou, Q., S. C. Yao, A. Russell, and J. Boyle. 1992. “Flue Gas NO_x Reduction Using Ammonia Radical Injection.” Journal of the Air & Waste Management Association 42(9): 1193–7.

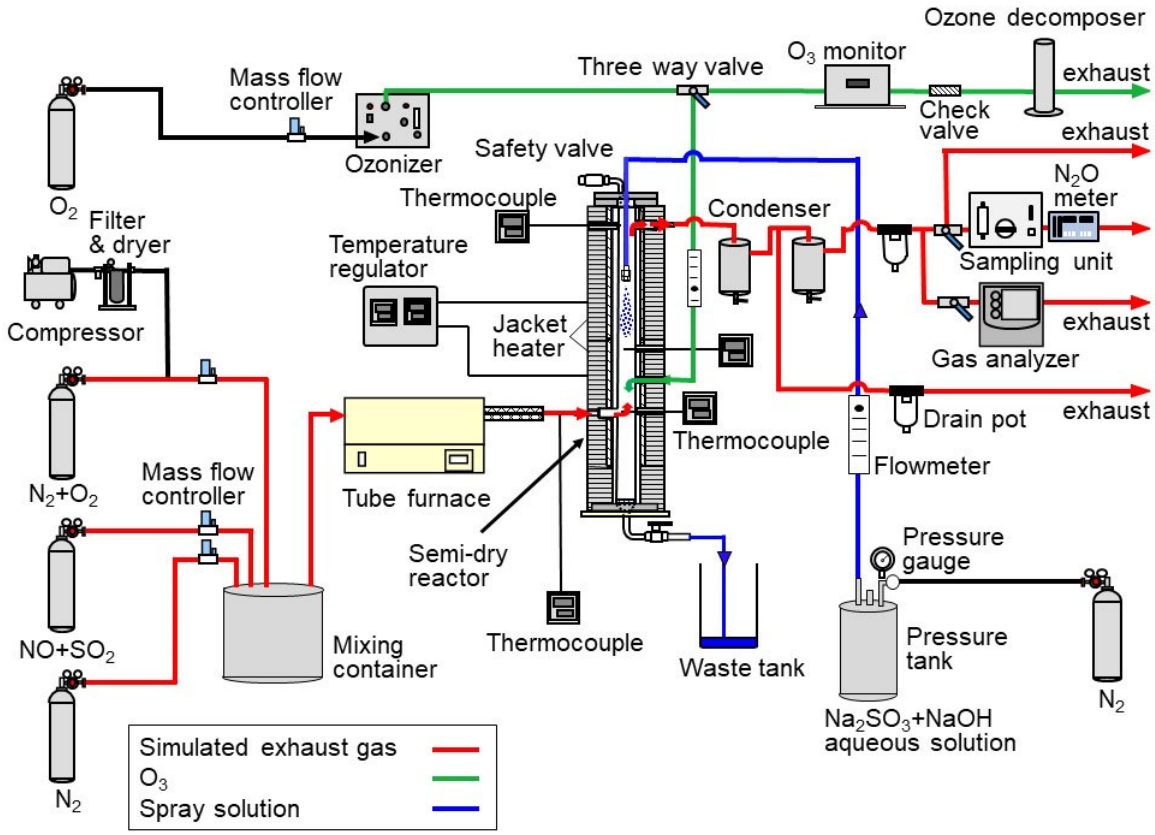

Figure 1. Schematic diagram of experimental set-up.

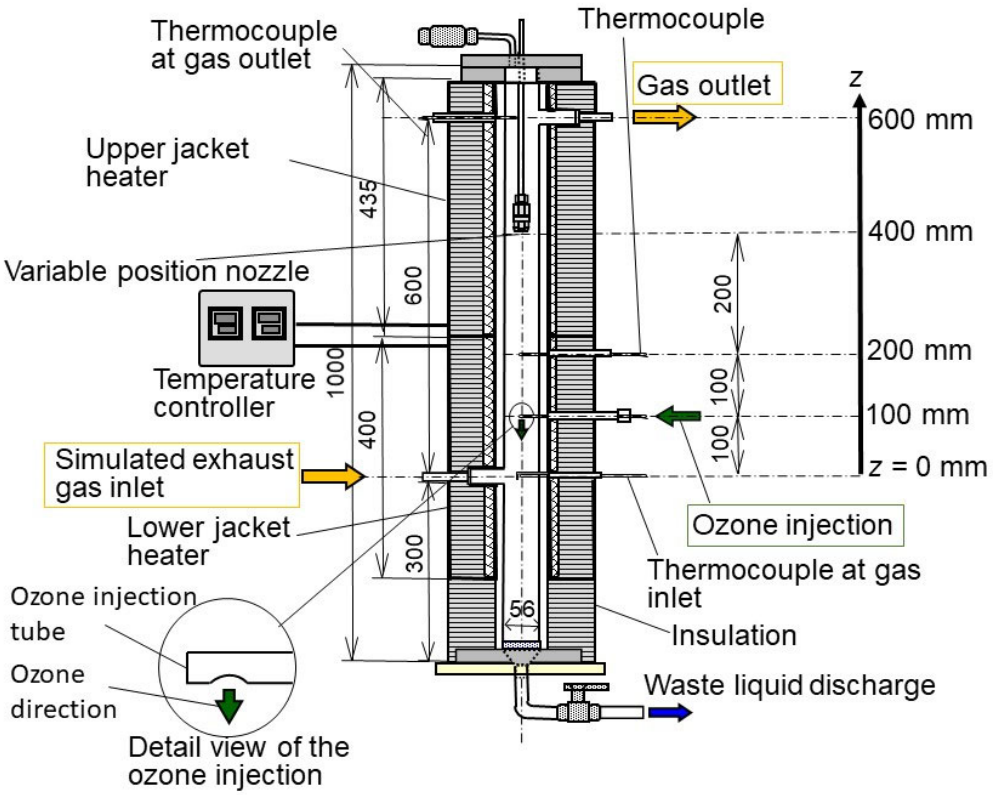

Figure 2. Detailed view of the semi-dry reactor.

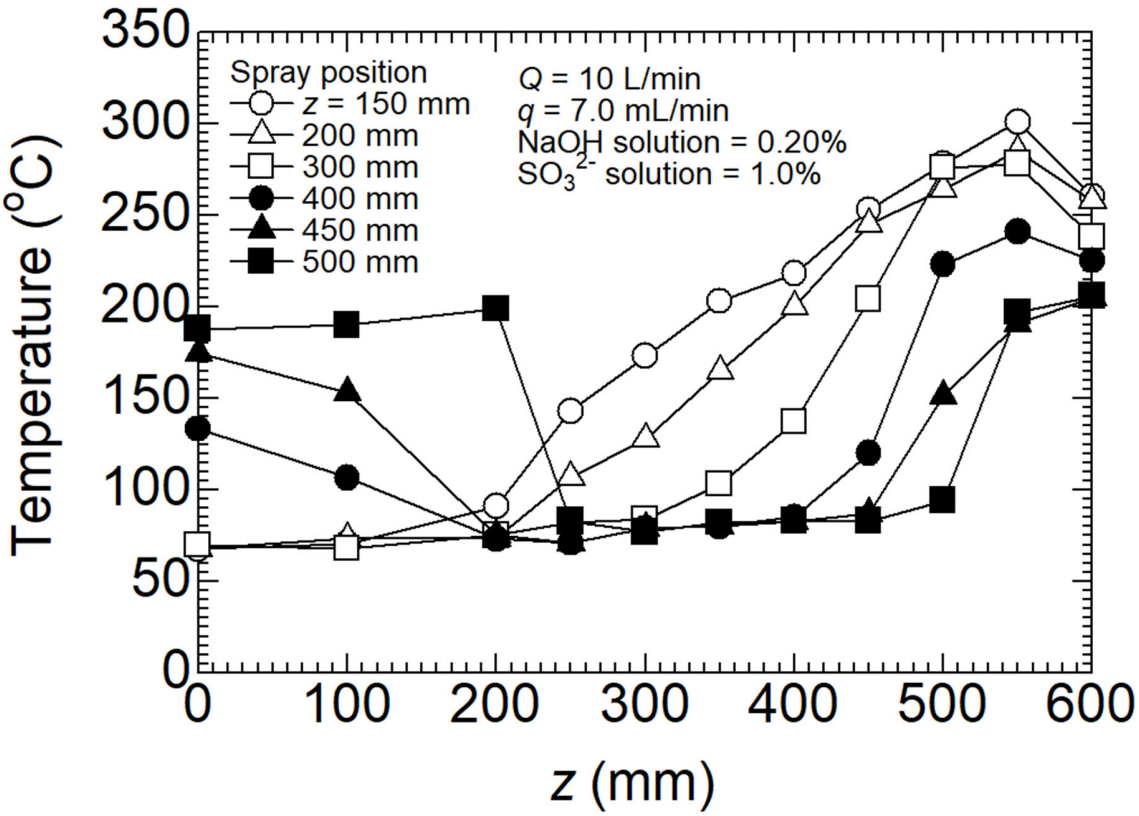

Figure 3. Temperature distributions of simulated exhaust gas at spray position of *z* = 150, 200, 300, 400, 450, and 500 mm.

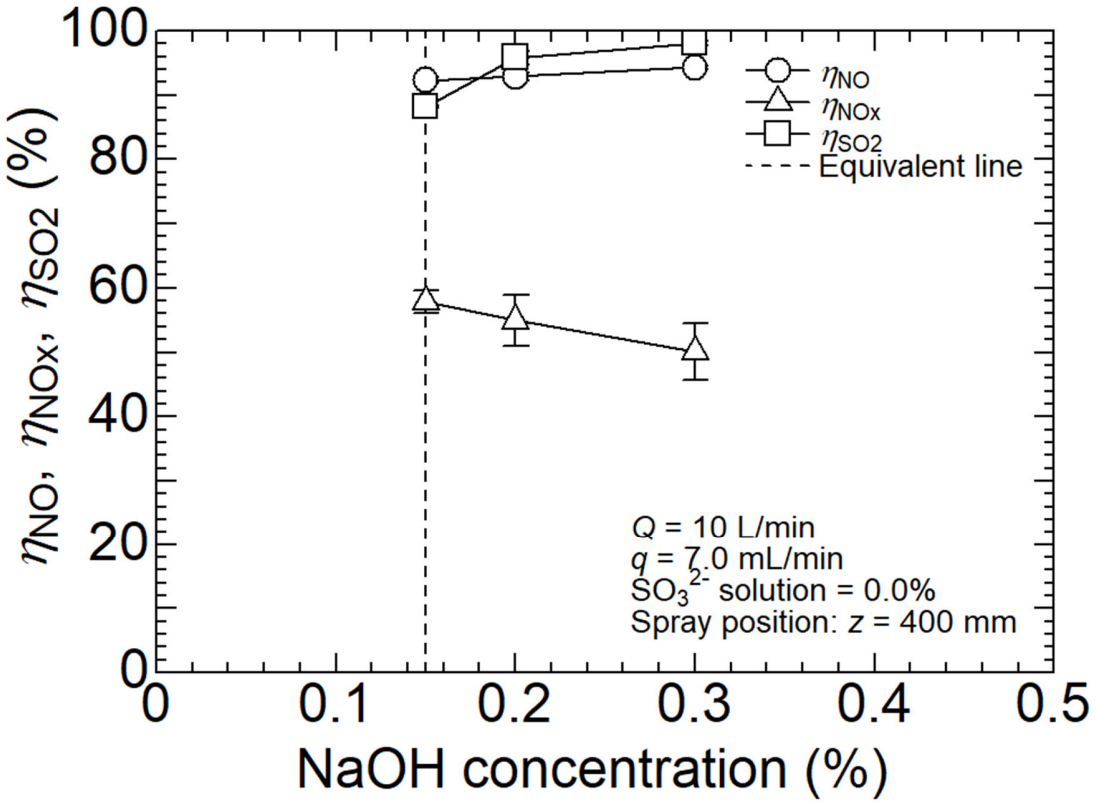

Figure 4. Removal efficiencies of NO (η_{NO}), NO_x (η_{NOx}), and SO_2 (η_{SO2}) as a function of NaOH concentration.

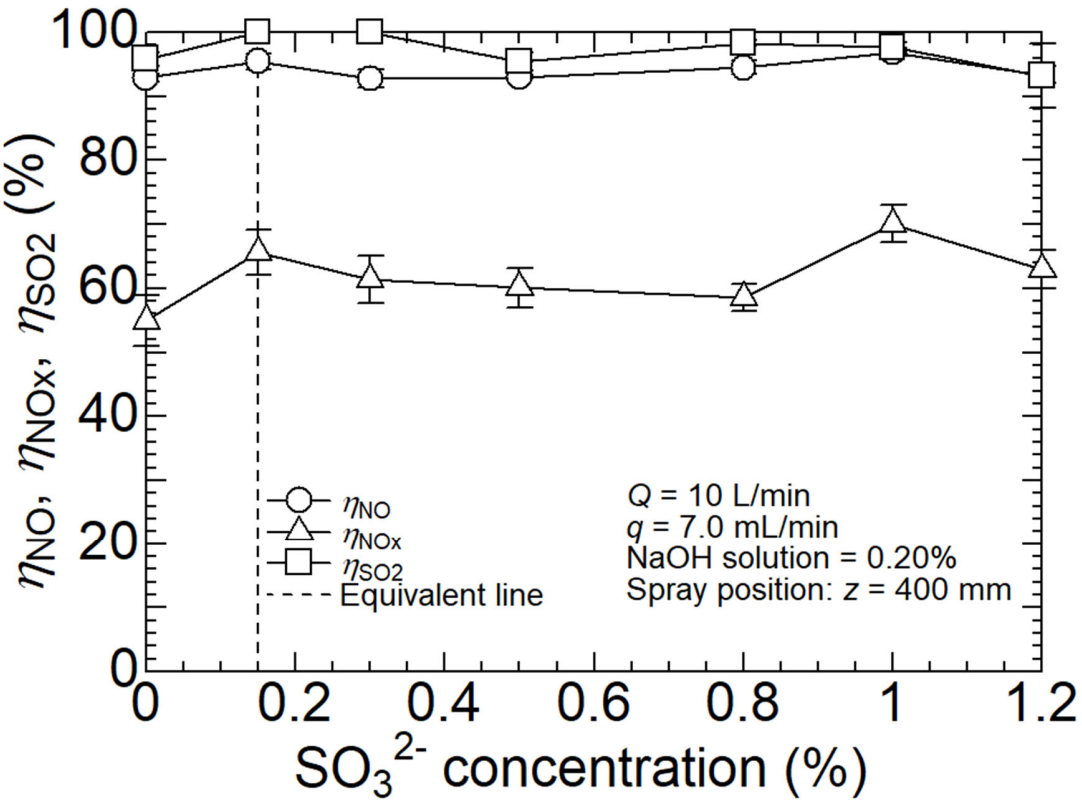

Figure 5. Removal efficiencies of NO, NO_x, and SO_2 as a function of SO_3^{2-} concentration.

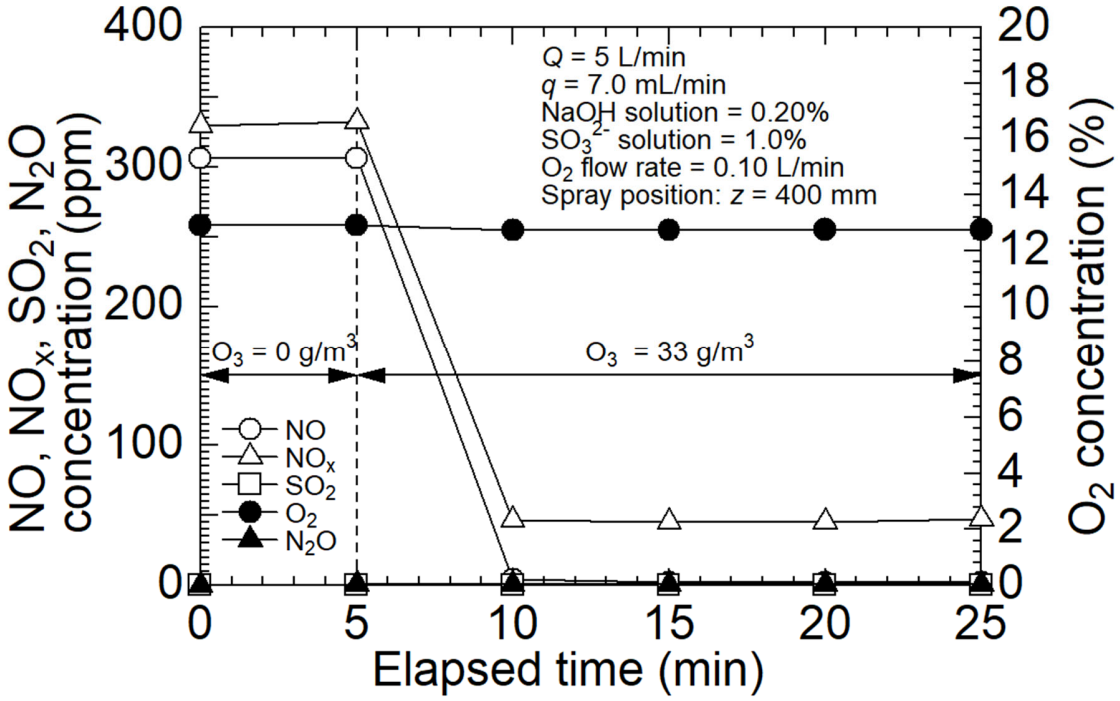

Figure 6(a). Time-dependent gas concentrations at Q = 5 L/min.

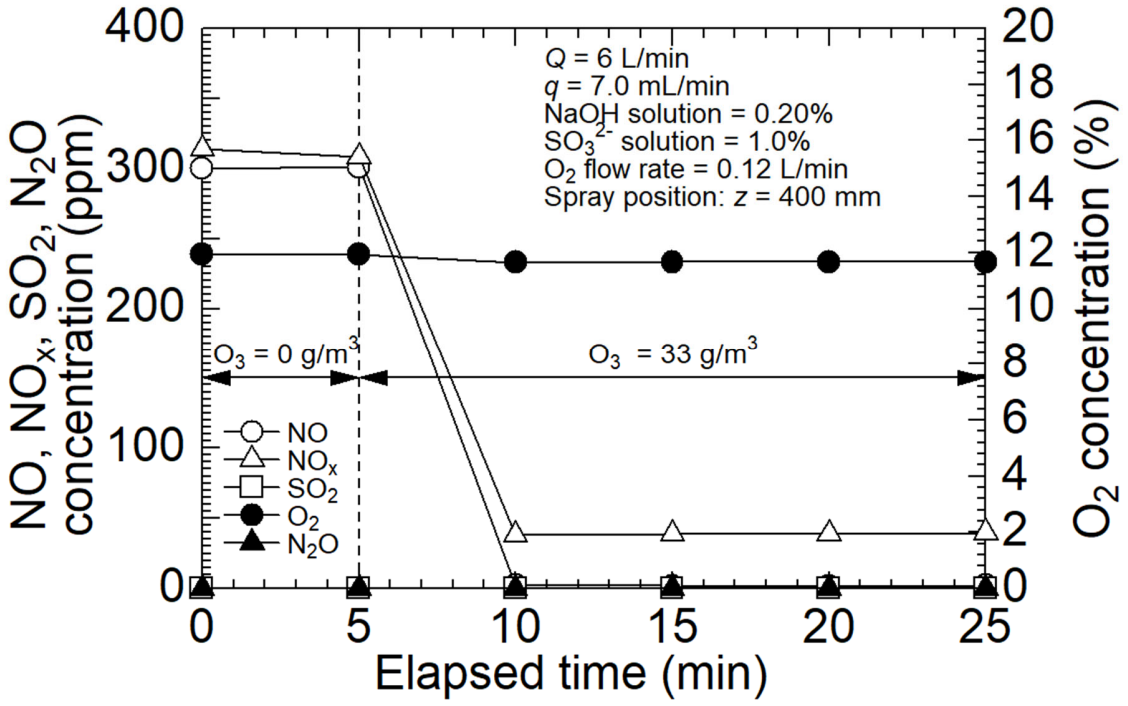

Figure 6(b). Time-dependent gas concentrations at Q = 6 L/min.

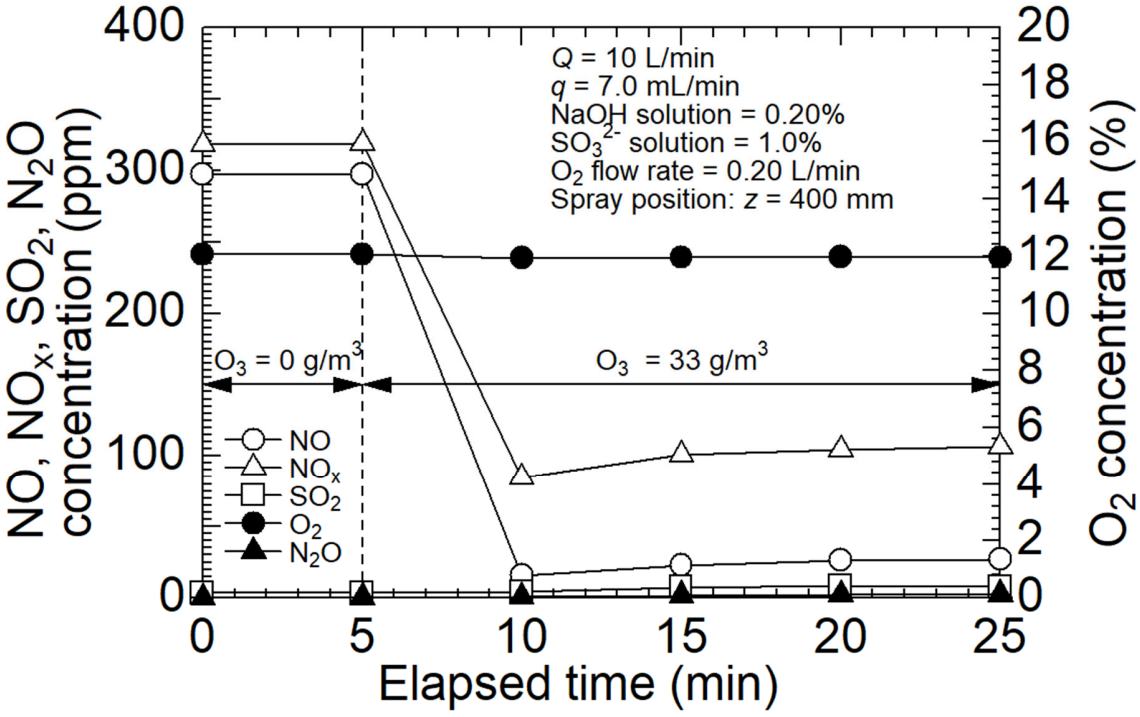

Figure 6(c). Time-dependent gas concentrations at Q = 10 L/min.

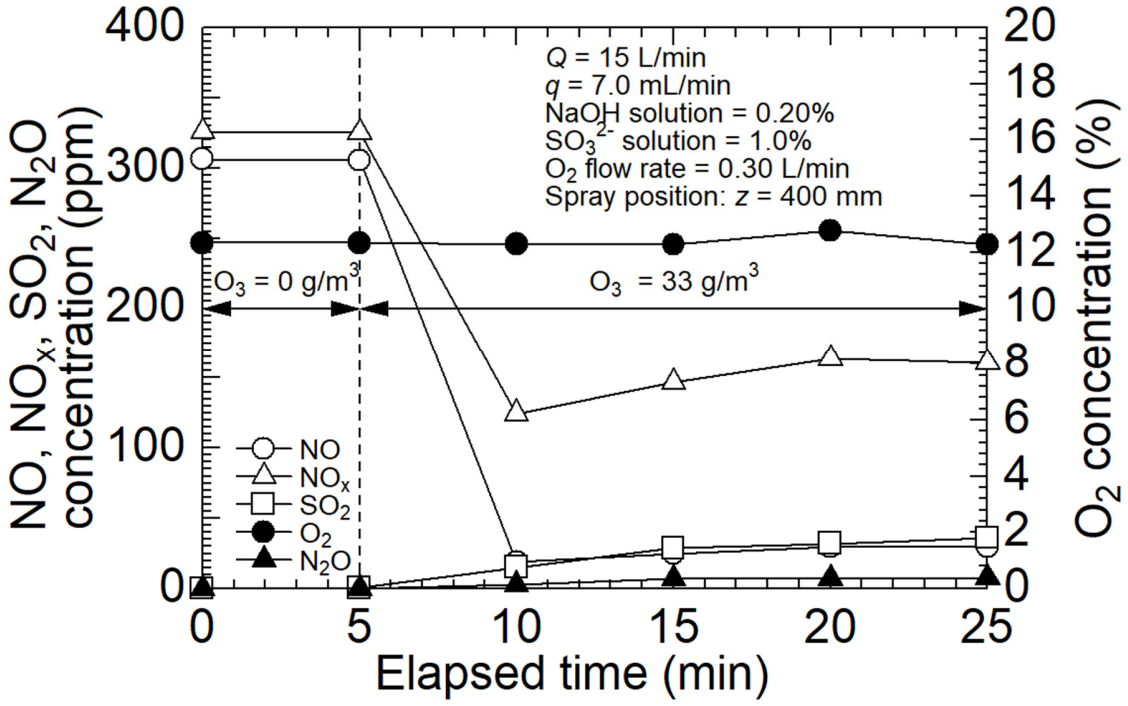

Figure 6(d)**.** Time-dependent gas concentrations at *Q* = 15 L/min.

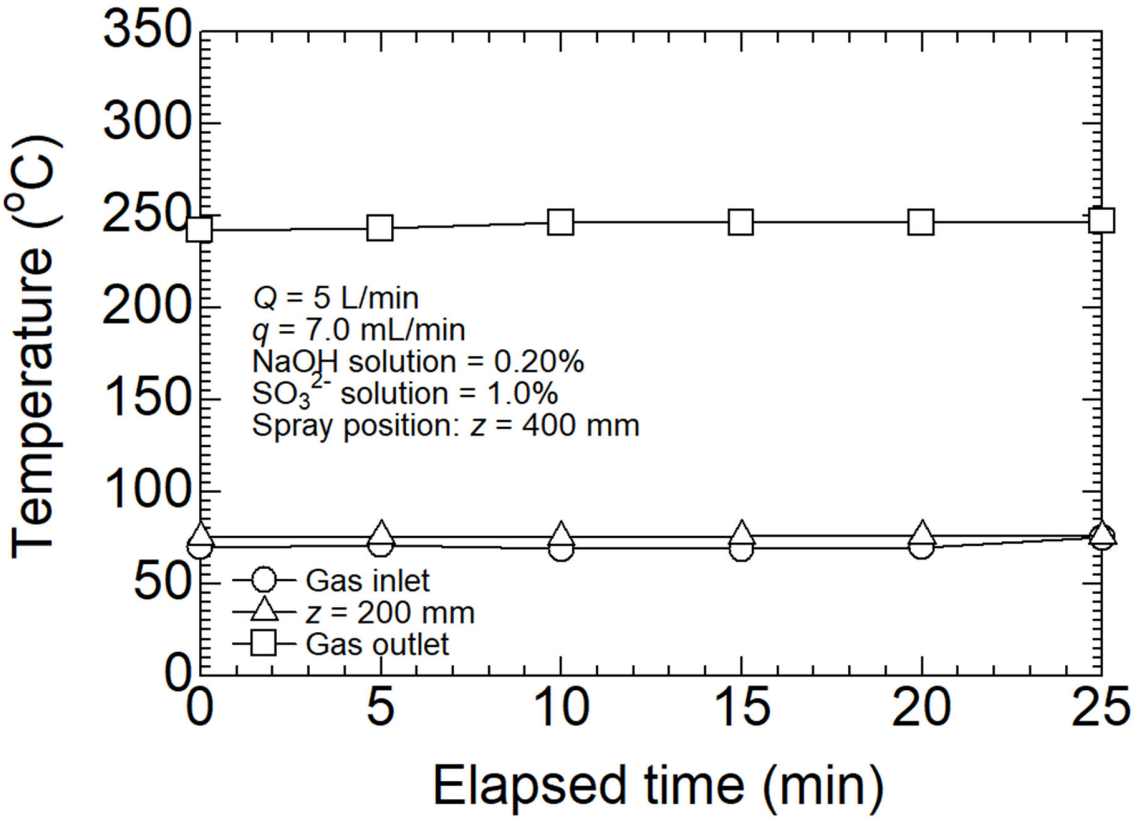

Figure 7(a). Time-dependent temperature at Q = 5 L/min.

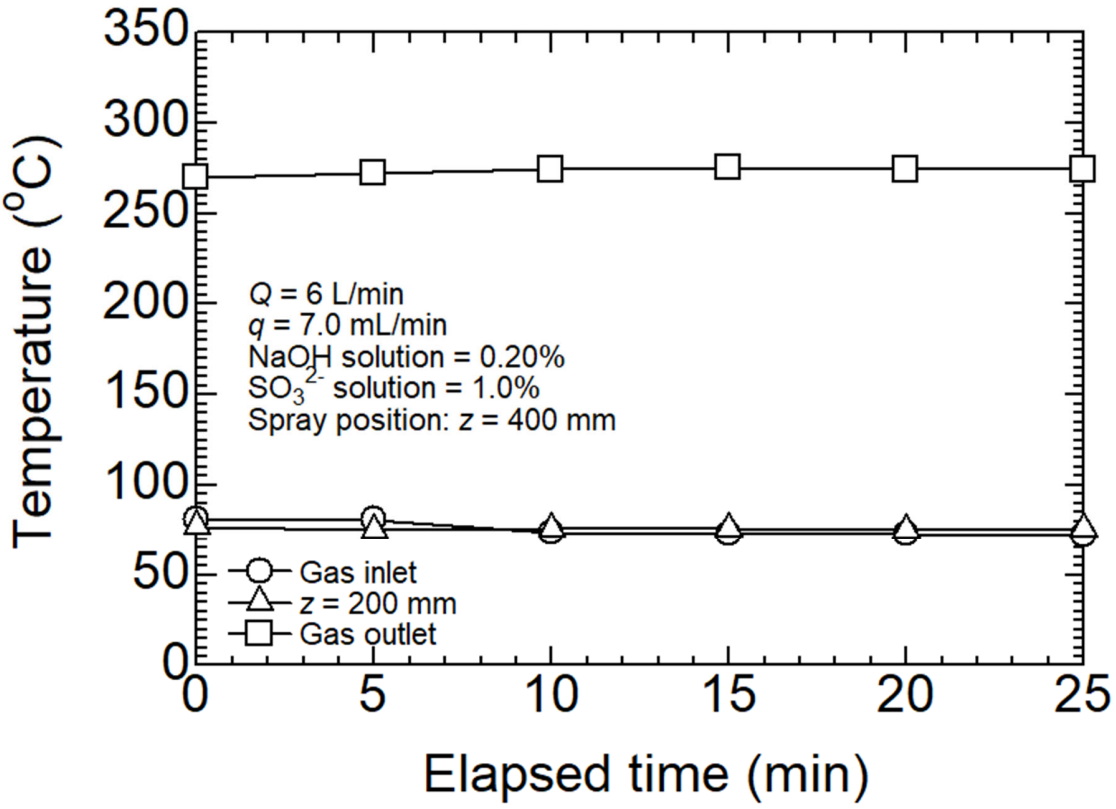

Figure 7(b). Time-dependent temperature at Q = 6 L/min.

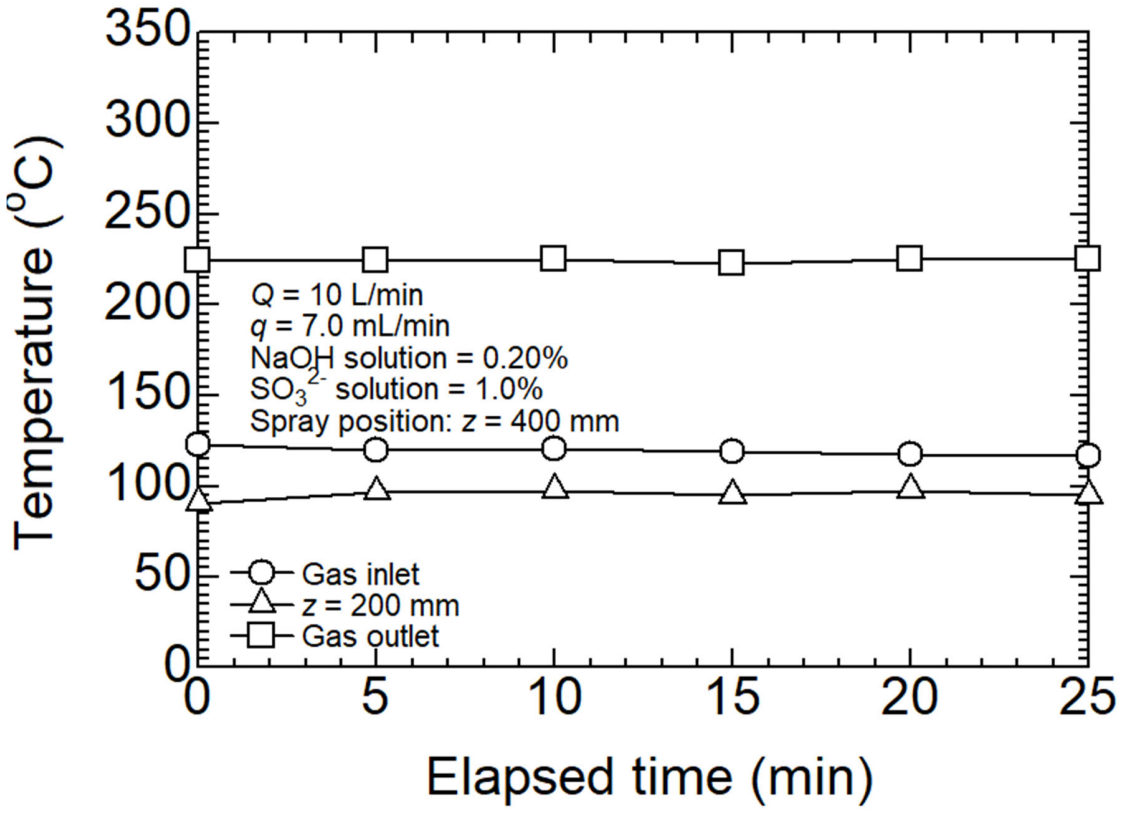

Figure 7(c). Time-dependent temperature at Q = 10 L/min.

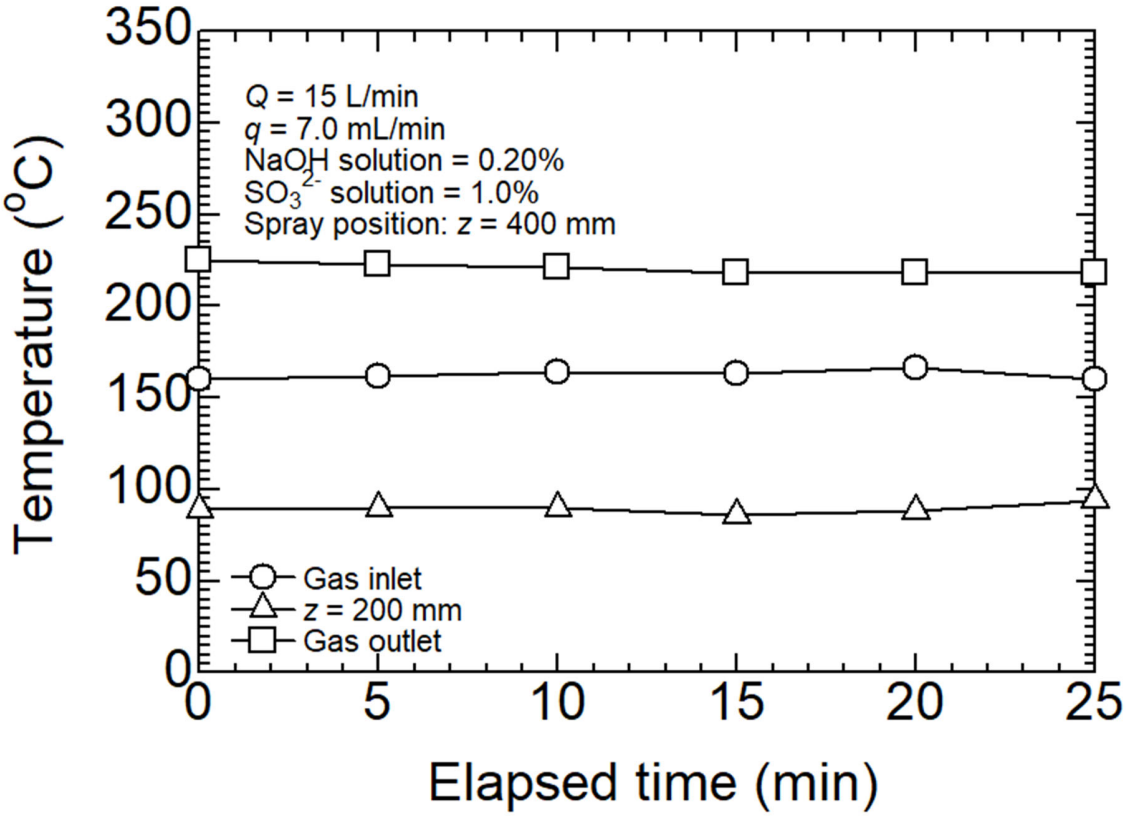

Figure 7(d). Time-dependent temperature at Q = 15 L/min.

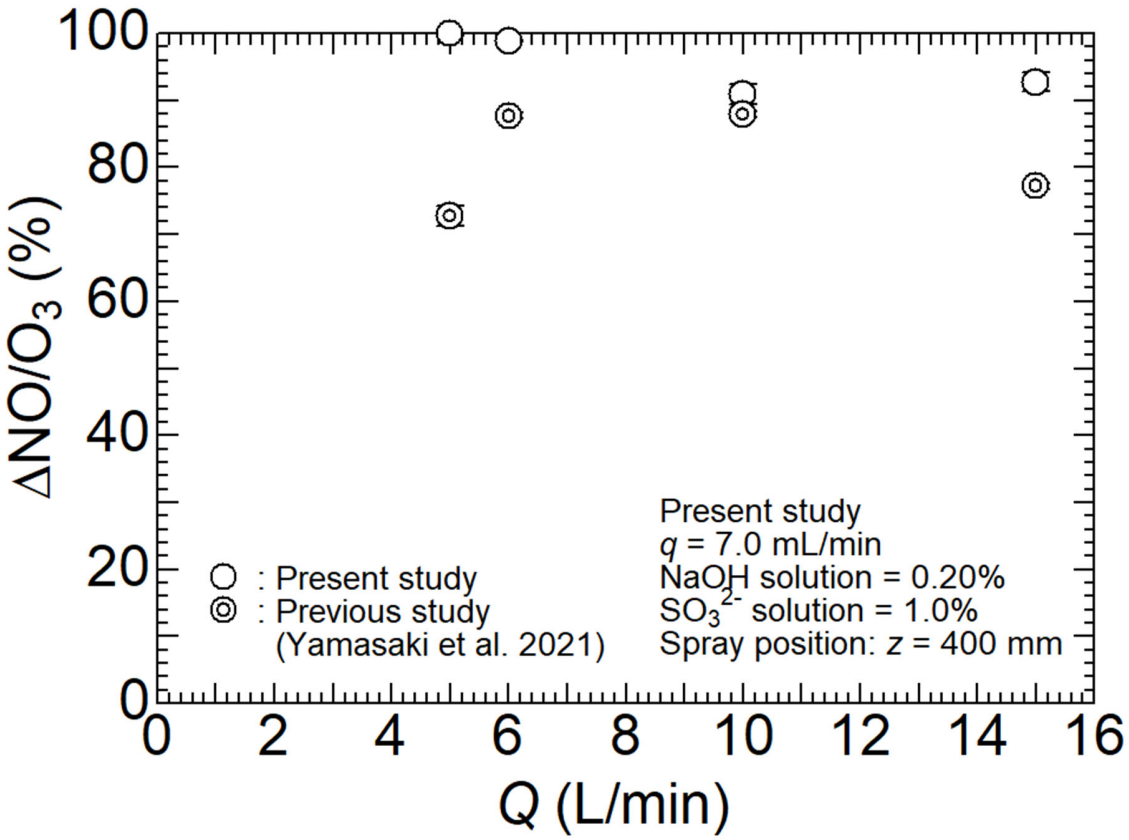

Figure 8. Δ NO/O_3 as a function of the flue gas flow rate.

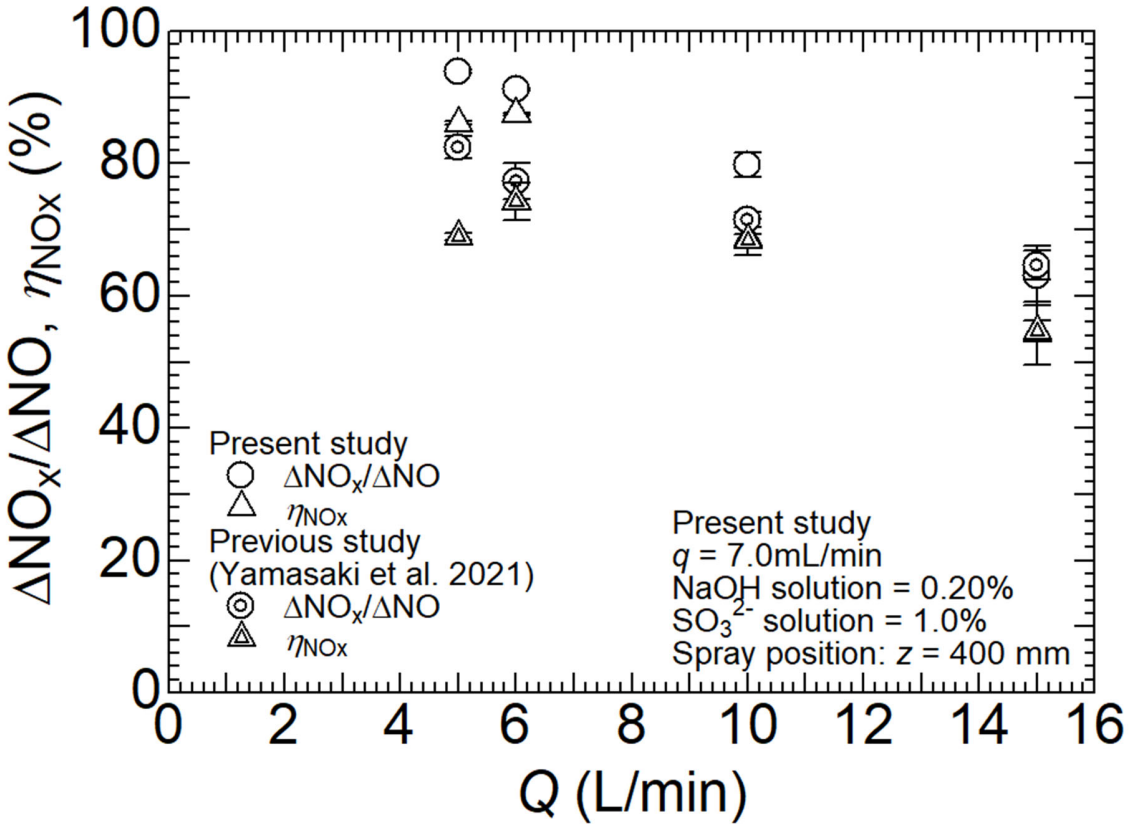

Figure 9. $\Delta NO_x/\Delta NO$ and NO_x removal efficiency as a function of the flue gas flow rate.